NASA TECHNICAL TRANSLATION

NASA TT F-11,666

NASA TT F-11,666

THE RESONANCE PROBE

Dimitri Lepechinsky, A. Messiaen, P. Rolland

Translation of "La Sonde a Resonance", Commissariat a l'Energie Atomique, Centre d'Etudes Nucleaires, Saclay, (France), CEA-R-2945, p. 31, 1966.

NATIONAL AERONAUTICS AND SPACE ADMINISTRATION
WASHINGTON, D.C. 20546 JULY 1968

THE RESONANCE PROBE

D. Lepechinsky, A. Messiaen, P. Rolland

ABSTRACT. The experimental findings of the report indicate satisfactory agreement with the theoretical expectations of Messiaen [14], Lepechinsky [16], and Rolland [17] concerning electron density as furnished by antiresonance, the thickness of the sheaths, and even the frequency of "neutral electron" collisions. The simplified theory of the authors is based on hydrodynamic equations with adequate limit conditions and accounts well for the essential phenomena observed. This holds true also for other problems of resonance of the same kind [10, 28, 29], provided conditions are such that non-collision damping is not destroyed by resonance which is certainly not random as stated recently in [30]. Experimentation to determine the limits of application of the simplified theory and to measure non-collisional effects is under way.

1. Introduction /3*

The method of the resonance probe consists in superposing a variable h-f voltage Φ_0 of frequency $\omega/2\pi$ on the direct voltage V_0 applied to the classical Langmuir probe. The curvature of the characteristic I (V) produces rectification which increases the direct current of the probe by a quantity δI_{cc} as a function of the h-f frequency. The increase δI_{cc} shows a maximum for a given angular frequency ω_R from which we can deduce certain characteristics of the plasma. The principal stages of the investigation of the h-f probe were as follows below.

Resonance was observed for the first time in 1960 by Takayama, Ikegami, and Miyasaki [1]. The theoretical study of Ichikawa and Ikegami [2], published in 1962, was based on an infinite-plane geometry where the sheath was neglected. In such a geometry, it was shown to be necessary to introduce a certain arbitrary length L of the penetration of the h-f field in the plasma. The model without sheath shows resonance at the plasma frequency ω_P which seemed confirmed by the work of

---

*Numbers in the margin indicate pagination in the foreign text.

Cairns [3] in 1963. This conclusion began to appear doubtful after 1963 from the investigations of Peter, Muller, and Rabben [4], Mayer [5], and Wimmel [6]. It appeared that the ion sheath plays an essential role which results in a resonance frequency $\omega_R < \omega_p$.

The only possibility of avoiding the introduction of the arbitrary length L would have been to select a model with a geometry for which field and potentials could effectively be calculated. This was the case of a model investigated by Vandenplas and Gould [7,8] in 1961. The model presented characteristics analogous to those of the probe and was constituted by a plane capacitor of which a part of the dielectric was formed by a section of plasma. It had a resonance frequency /4
of $\omega_R < \omega_p$ and further an antiresonance frequency $\omega_A = \omega_p$.* The conclusions of Vandenplas and Gould [7,8] were experimentally confirmed in [10,11]. Mayer [5] utilized this model for qualitative explanation of the author's experimental findings, although obtained with a plane probe and consequently a rather different geometry. In 1964, Harp and Crawford [12] carried out a qualitative study of the erical probe in which the numerical data of Pavkovich and Kino [13] concerning the penetration of a h-f field in a plasma limited by an infinite plane were adapted to the spherical case by the introduction of a correction factor providing for decrease of the h-f field in $1/r^2$. In this study, the thickness of the sheath is arbitrarily estimated as 5λ (λ = Debye shielding distance) and the antiresonance phenomenon does not appear explicitly.

The theory proposed in 1964 by Messiaen [14] is based on the resolution of a problem with adequate limit conditions for the resonator constituted by the probe, the sheath and the plasma. No arbitrary parameter is introduced and the sheath is estimated from the solution of the static problem [15].

This method is in principle applicable to any probe geometry for which the solution of the Laplace equation is cancelled in the infinite and to the extent where the dimensions of the probe are small in regard to the wavelength in vacuum. This theory together with its extensions and limits [16,17], is summarized in Section 2.

The experimental findings on resonance obtained by other /5
laboratories [12, 18, 19] agree qualitatively with our theoreti-

---

*It appeared also that the principal characteristics of this system are very little modified by the electron temperature. The latter gives rise to a subsidiary resonance spectrum for $\omega > \omega_p$ which is observed when ν/ω is small [10].

cal expectations. We present here a quantitative comparison of these expectations with our experimental results regarding resonance, antiresonance, electron density, Debye shielding distance, thickness of the sheath, and the frequency of collisions.

The effect of transit time in the sheath and non-collision damping which were investigated in [17] are capable of greatly affecting the amplitude of resonance and an experimental investigation of these effects is under way.

2. Theory of the Spherical Resonance Probe

Let us consider a metallic body submerged in an infinite plasma and brought to a continuous potential $V_0 < o$ in relation to the plasma potential. This potential and the geometric form of the probe determine the distribution of electron density of the near environment of the probe in view of the appearance of an ion sheet separating the probe from the non-disturbed plasma. Let us further consider the effect of a h-f voltage Φ_0 (such that $|\Phi_0| << |V_0|$) additionally applied to the probe by limiting ourselves to the case where the frequency of the h-f signal is such that the wavelength is very much larger than the dimensions of the latter. This hypothesis makes it possible to arrive at a "quasi-static" approximation for describing the electric field $\vec{E}$ around the probe. This amounts to stating $\vec{E}$ = - grad Φ and makes it possible to reduce the electromagnetic to an electrostatic problem for satisfactory description of this field in the close vicinity of the probe, and consequently, to derive the h-f current corresponding to the h-f voltage applied. We also assume that, in the plasma under consideration, the h-f motion of the ions is negligible in relation to that of the electrons and that only the latter contribute to the resonance effects. In order to obtain an approximate solution of the problem, we shall consider the plasma as cold and describe it by its equivalent permittivity which permits a sufficiently accurate description of the dominant effects. Since we are in the presence of two problems of electrostatics under these conditions, we must first solve the Poisson equation in order to obtain the profile of electron density N_e around the probe and subsequently treat the electromagnetic problem in this medium by a "quasi-static" approximation. This can be done easily only for the simple probe geometry. It is then possible to utilize a system of natural coordinates of the arrangement under consideration which will easily express the limit conditions. /6

The numerical solution of the Poisson equation for determining the density profile in the sheath has been given by several authors for the plane, cylindrical and spherical geometry on the basis of certain simplifying hypotheses on ion motion [20, 21, 22, 23]. It appears that the electron density decreases very rapidly at a very short distance from the probe and becomes very low in the immediate vicinity of the latter. This fact allows us to approach the continuous variatio us to approach the continuous variation of density by a discontinuous variation in order to obtain an analytical solution of the h-f problem. We shall suppose that, in the sheath, the electron density is negligible and that, outside of the sheath, it has the value N_{eo} corresponding to the non-disturbed plasma. The thickness of the sheath will be estimated from the numerical solution of the Poisson equation by defining the sheath-plasma boundary by the condition $N_e = N_{eo}/2$.

The h-f field is assumed to have the form $e^{-i\omega t}$, and can /7
then be obtained by solving the Laplace equation in the media considered with adequate expression of the limit conditions ($\Phi = \Phi_0$ on the probe; $\Phi = 0$ to ∞; continuity of potential and of the component of the electric-shift vector normal to the boundary surface sheath-plasma). We must therefore select, for the h-f resonator consisting of the system of probe, sheath and plasma, a geometry making it easily possible to express these conditions (accordingly, a plane probe constituted by a disc will be assimilated to a flattened spheroid and a sylindrical probe to an elongated spheroid).

a) Solution of h-f Problem

We shall discuss in detail only the spherical probe. The reader will find in [14] the calculations for the plane and cylindrical case which are treated identically. We shall here neglect the effects due to reflection of electrons from the sheath and assume that only scattering results from collision.

Let a be the radius of the probe and b = a + g that of the sheath. Our system of spherical coordinates r, θ, ϕ will be centered in the center of the probe. The permittivity of the sheath, assumed to be empty, will be ε_0; that of the plasma surrounding ε_p and assumed to be homogenous and isotropic, shall be such that

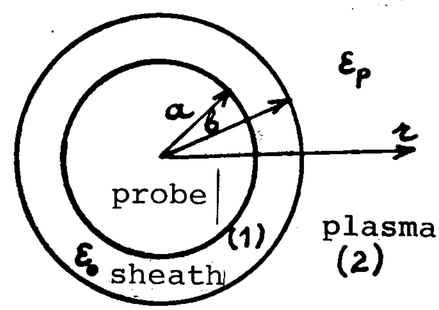

Fig. 1

$$\varepsilon_p/\varepsilon_0 = 1 - \frac{\omega_p^2}{\omega^2}\frac{1}{(1 + i\nu/\omega)} \qquad (1)$$

where ν is the frequency of collision.

The different media are assumed to be electrically neutral /8
so that the Poisson equation is reduced to that of Laplace and we can write in spherical coordinates (with $\frac{\delta}{\delta\theta} = \frac{\delta}{\delta\phi} = 0$ by reason of symmetry):

$$\nabla^2\phi = \frac{1}{r^2}\frac{d}{dr}\left(r^2\frac{d}{dr}\phi\right) = 0 \qquad (2)$$

The h-f solution in media (1) and (2) will be:

$$\Phi_1 = A + B/r \quad \text{et} \quad \Phi_2 = C/r.$$

The limit conditions in r = a and r = b give the relations

$$\begin{cases} A + \frac{B}{a} = \Phi_0 & \text{(h-f potential applied to the probe)} \\ A + \frac{B}{b} = \frac{C}{b} & \text{(continuity of potential in } r = b\text{)} \\ -\varepsilon_0 \frac{B}{b^2} = -\varepsilon_p \frac{C}{b^2} & \text{(continuity of the normal component of shift } D = \varepsilon E \text{ in } r = b\text{)} \end{cases} \qquad (3)$$

and make it possible to fully solve the problem.

Specifically, the density of the h-f current collected by the probe is given by

$$J_{HF} = \varepsilon_0 \frac{\partial \vec{E}}{\partial t} = i\omega\varepsilon_0 \frac{B}{a^2} = \frac{i\omega\varepsilon_0}{a^2}\Phi_0 \frac{\frac{\varepsilon_p}{\varepsilon_0}\frac{ab}{b-a}}{\frac{\varepsilon_p}{\varepsilon_0} + \frac{a}{b-a}} \qquad (4)$$

Accordingly, it appears that, when $\nu/\omega \ll 1$, J_{HF} passes through a maximum for $\omega = \omega_R < \omega_p$ as given by

$$\omega_R = \omega_p \sqrt{\frac{b-a}{b}}\ ^* \qquad (5)$$

and through a minimum for $\omega = \omega_p$. The general rate of variation of J_{HF} with frequency is shown in Fig. 2 (for $\nu = 0$).

The maximum value of J_{HF} which is infinite in the absence of collision, is a function of this in accordance with the following approximate relation: /9

$$J_{HF(max)} \cong -\frac{\varepsilon_0 \omega_p^2 \Phi_0}{\nu b} \qquad (6)$$

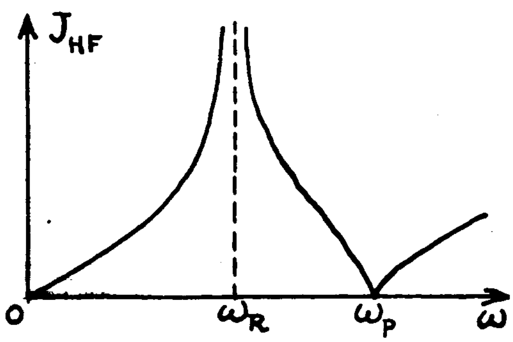

Fig. 2

---

*For a plane or cylindrical probe, the findings obtained are analogous [14]; the h-f current passes through a maximum for $\omega_R = \omega_p \theta$ (with $0 < \theta < 1$) where θ is a function only of the system geometry, and through a minimum for $\omega_A = \omega_p$.

b) Solution of the Problem of Direct Current of the Probe

We know that the classic theory of the Langmuir probe leads to the following relation for the density of the electronic current collected by the probe at a negative potential V_o in relation to the plasma potential

$$j_e = j_s \exp(eV_o/KT_e), \tag{7}$$

where K is the Boltzmann constant and

$j_s = ne(KT_e/2\pi m)^{1/2}$ = density of the electronic-saturation current.

If we superpose, on the direct potential V_o, an ac-potential $\delta\Phi_g \sin\omega t$, then the mean value in time of the electronic current reaching the probe is given, neglecting the transit time of the electrons in the sheath, by

$$\bar{j}_e = j_s \overline{\exp(eV'/KT_e)} \quad \text{with} \quad V' = V_o + |\delta\Phi_g|\sin\omega t,$$

i.e.

$$\bar{j}_e = j_s\{\exp(eV_o/KT_e)\}\frac{1}{T}\int_0^T \exp\left(\frac{e|\delta\Phi_g|}{KT_e}\sin\omega t\right)dt \tag{8}$$

with

$$T = \frac{2\pi}{\omega},$$

that is

$$\bar{j}_e = j_s\left\{\exp\frac{eV_o}{KT_e}\right\} I_o\left(\frac{e\delta\Phi_g}{KT_e}\right), \tag{9}$$

where $I_o(x)$ is the modified Bessel function of the first kind and of zero order.

With Boschi and Magistrelli [24], we are assuming that the plasma is not disturbed until the boundary of the sheath in which the potential difference $V_o + \delta\Phi_g \sin\omega t$ exists. Accordinly, we must calculate $\delta\Phi_g = \int_{\text{sheath}} \vec{E}\, d\vec{l}$ on the basis of the solution of the h-f problem and will then obtain. /10

$$\delta\Phi_g = \frac{B}{b} - \frac{B}{a} = \Phi_o \frac{\varepsilon_p/\varepsilon_o}{\varepsilon_p/\varepsilon_o + \frac{a}{b-a}} \tag{10}$$

It will be easily seen that only this difference of potential is subject to the effects of resonance and antiresonance, for the same reason as the current J_{HF} evaluated above, and that ω_R and ω_A are the same for both parameters.

A series of development of $I_o\left(\frac{e|\delta\Phi_g|}{\mathcal{K}T_e}\right)$ appears in (19) and leads through increase $\delta J_e = \delta I_{cc}/S$ of the direct current of the probe to the expression

$$\frac{\delta I_{cc}}{S} \simeq \frac{1}{4}\left(\frac{e|\delta\Phi_g|}{\mathcal{K}T_e}\right)^2 j_e \;, \tag{11}$$

where J_e is given by (7) when $e|\delta\Phi_g|/\mathcal{K}T_e < 1$, and S is the surface of the probe. (9) shows that, for sufficiently negative polarization, j_e tends toward zero as well as δI_{cc} given by (11). The rate of variation of δI_{cc} as a function of ω/ω_p for a given sheath thickness and derived from Rel. (11) is shown in Fig. 3.

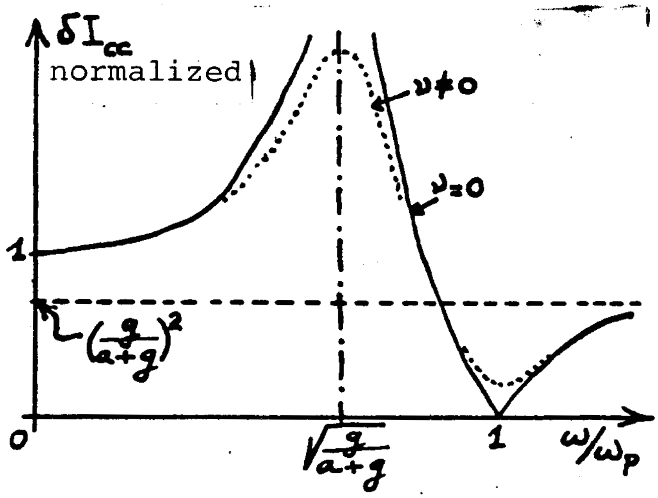

Fig. 3

When we utilize Rel. (10) and (11), it is easy to see that:

1) the ratio of R of the amplitude of the peak of resonance to that of δI_{cc} or $\omega\to 0$ is given by the expression

/11

$$\mathcal{R} = \frac{\delta I_{max}}{\delta I_{(\omega=0)}} = \left(\frac{\delta\Phi_g}{\Phi_o}\right)^2_{max} = \frac{a^2(b-a)}{b^3}\,\frac{\omega_p^2}{\nu^2} \;, \tag{12}$$

which allows us to derive the frequency of collision ν as a function of ω_p and the thickness of the sheath. When we introduce the parameter $\omega_R = \omega_p\sqrt{\frac{b-a}{b}}$, (10) is written as

$$\frac{\delta\Phi_g}{\Phi_o} = \frac{1}{1 + \dfrac{\omega(\omega+i\nu)(\omega_p^2-\omega_R^2)}{\omega_R^2\left[\omega(\omega+i\nu)-\omega_p^2\right]}} \;; \tag{13}$$

When $\nu < \omega_R < \omega_P$, then the square of the modulus of this function has a maximum for $\omega \approx \omega_R$. The value of this maximum is

$$\mathcal{R} = \left(\frac{\delta\Phi_g}{\Phi_0}\right)^2_{max} \simeq \frac{\omega_R^2(\omega_P^2 - \omega_R^2)^2}{\nu^2 \omega_P^4}, \tag{14}$$

and is an expression identical to (12);

2) the ratio varies as a function of sheath thickness g (and consequently as a function of direct plarization V_O) and passes through a maximum for a well defined value of g [16]. The maximum R is reached for

$$\omega_R \simeq \frac{\omega_P}{\sqrt{3}}, \tag{15}$$

and amounts to $\mathcal{R}_{MAX} = \left(\frac{\delta\Phi_g}{\Phi_0}\right)^2_{mm} \simeq \frac{4}{27}\left(\frac{\omega_P}{\nu}\right)^2.$

which corresponds to a sheath thickness $g = b - a \cong a/2$.

When $\omega_R < \nu$, the maximum disappears. The module of Function (13) is then on the order of ω_R/ν in $\omega = \omega_R$. Resonance then no longer exists.

Fig. 16 gives the rate of the module of (13) for six values of ω_R/ω_P. We see that the relative amplitude of the resonance decreases when $|V_O|$ increases (thick sheath: $\omega_R \to \omega_A$) and when $|V_O| \to o$ (the sheath disappears).

Formula (15) makes possible in principle direct measurement of ω_P and Rel. (14) shows that measurement of R_{max} allows us to determine the frequency of collision ν. It should be noted that there exists in principle another way of liberating ourselves from knowledge of the sheath, i.e. by utilizing two different probes [12] or the same probe with several polarizations. We then proceed by successive approximation in using the findings of [15]. /12

c) Non-Collision Effects

Two types of non-collision phenomena may profoundly modify the amplitude of resonance, to wit: (a) reflection of the electrons from the sheath which produces a mixture of energy-dissipating phases and reduces h-f resonance, i.e. J_{HF} given by (4) and $\delta\Phi_g$ given by (10) as well as subsequently direct resonance, i.e. δI_{CC} given by (11); (b) the transit time of the electrons in the sheath whose phases intermix and produce a decrease of direct resonance characterized by δI_{CC}. Under our experimental conditions, these phenomena were generally of little importance as shown in a simplified theoretical study [17]. However, a systematic experimental investigation of these effects is under way.

3. Experimental Verification

a) Experimental Arrangement

We utilized a diffusion plasma of mercury vapor produced by two lateral discharges in a sealed spherical balloon of pyrex with a diameter of 30 cm. The lateral discharges are contained each in a lateral "ear" of the balloon arranged at /13 the sides and have the same diameter (cf. Fig. 4). Each is constituted by a barium and strontium-coated filament (heated to 800° C by rectified current) and by a cylindrical nickel plate with a diameter of 4 cam surrounding the filament. Heated in parallel the two filaments are brought to nagative dc voltage in relation to the plates. The plate current is controlled by a rheostat and the feed voltage. Accordingly, the discharge current in each ear can be adjusted independently between zero and 2.5 A. An anode-filament voltage of some 10 V is necessary to initiate the discharge.

Since both discharges are radial, the plasma entering the balloon is a diffusion plasma where the arrangement of the filament and the plates produces an electric field perpendicular to the direction of penetration in the balloon and here provides for a quasi-Maxwell distribution of the electrons in the range of the discharges utilized.

A spherical probe of stainless steel with a radius of 2 cm. is located in the center of the balloon and supported by the center rod of a coaxial in such fashion that the h-f signal is applied to the plasma only through the spherical surface of the probe. The driving coaxial is insulated from the plasma by a pyrex tube.

Two additional cylindrical probes have been provided, one at half-radius and the other toward the wall of the balloon for secondary controls. A nickel grid was also inserted at the output end of one of the ears in order to make the plasma as symmetrical as possible in the balloon.

Prior to sealing, the balloon was exhausted by prolonged /14 vacuum pumping during which the thermionic cathodes were activated in customary manner. At a residual pressure of about 10^{-6} mm. Hg, a few drops of mercury were introduced in the balloon and the latter sealed. Accordingly, the pressure in the balloon is equal to that of the mercury-vapor tension at ambient temperature [25].

Toward 15° C when pressure is on the order of a micron, the number of neutral molecules in the balloon is about 3.9 x 10^{13} per $cm.^3$ and the mean free path of "neutral neutrons" and "neutral electrons" is on the order of a few cm. and varies inversely to pressure. Measurement of electron density and plasma temperature obtained with different discharge currents was made by the static method of the classic Langmuir probe and compared with the h-f method. The "static" measurements were made by applying to the spherical probe a variable potential furnished by a battery and by recording the resulting probe current on an XY-recorder. The variation of tension was made manually by means of a stepdown potentiometer.

The "h-f" measurements were made with the aid of a Wobbulator with a sweep between zero and 80 Mc/s at a rate of 50 times per second. The signal of the Wobbulator was amplified by two wide-band amplifiers in order to obtain a h-f voltage between 2 and 3 V. The spherical probe was energized by h-f across an impedance transformer of the type "cathode follower" and the high-frequency current measured by radiation with the aid of a loop antenna around the balloon. The h-f voltage induced in the loop was read from an oscilloscope after previous amplification by an appropriate H.F. slide wire.

The direct current of the probe passes through the polarization cell and is applied across a resistor and a capacitor to a wide-band low-frequency slide wire of the above oscilloscope and displayed on the second time base of the latter. This made it possible to simultaneously obtain the variation of J_{HF} and of δI_{CC}, as a function of the frequency applied, for each value of the discharges. The experimental arrangement is shown in Fig. 4. /15

b) Static Measurements

1. The Theory of the Langmuir Probe [26]

The current I collected by an electrode submerged in a plasma and polarized at a variable static potential V_o ($V_o = 0$ corresponding to the plasma potential) is the sum of the electronic (I_e) and ionic (I_i) currents where we can distinguish the characteristics $I_e = f(V_o)$ and $I_i = f(V_o)$.

(i) - Electronic Characteristic

If the electrons are in thermodynamic equilibrium at temperature Te, and $V_o \leq 0$, we have

$$N_e = N_{eo} \exp(eV_o/KT_e)$$

and Rel. (7) for the density of the electric current reaching the probe. When $V_o > 0$, J_e no longer obeys rule 7 but increases slightly with V_o (formation of an electronic sheath and increase of the effective surface of electron collection). From the representation of $\log I_e = f(V_o)$, we can determine Te, N_{eo} and the plasma potential $V_o = 0$. The floating potential V_w is defined for $|I_i| = |I_e|$.

(ii) - Ionic Characteristic /16

When $V_o < 0$, the ions are no longer characterized by a Maxwell distribution around the probeand fall freely on the latter to form a positive space charge characterizing the sheath. It is assumed that the mean free path of the ion is always large in relation to the thickness of the sheath. In general, the ion current I_i and the structure of the sheath can be obtained only by numerical solution of the Poisson equation

$$\nabla^2 V = -\frac{e}{\varepsilon_0}(N_i - N_e),$$

where V = potential in the plasma (= V_o on the probe).

A detailed review of the hypotheses and methods of solution was given in [15]. In the following, we utilize the numerical results based on the theories of Allen, Boyd and Reynolds [21] and Bernstein and Rabinowitz [20] where thermal excitation of the ions is neglected. Let us note that our experimental results also afford an indirect verification of these theories. For a spherical probe, the Poisson equation presents itself in the short form

$$\frac{1}{J}\frac{d}{d\xi}\left(\xi^2\frac{d\eta}{d\xi}\right) - \eta^{-1/2} + \xi^2 e^{-\eta} = 0,$$

or

$$\eta = \frac{eV}{KT_e} \quad ; \quad J = \frac{i_i}{I_\lambda} = \frac{I_i}{eI_\lambda} \quad ; \quad \xi = \frac{r}{\lambda_D} \quad ; \quad I_\lambda = \frac{KT_e}{e^2}\left(\frac{2KT_e}{m_i}\right)^{1/2}.$$

Chen [15] gives the numerical solution of this equation in the form of a system of curves (Figs. 5, 6) which expresses the relation between I_i, V, Te and the distance r from the center of the probe. We utilized this diagram for determining the Debye /17
distance and the thickness of the sheath.

Determination of λ_D: for a given potential of the probe V, we calculate η since Te is already known from the electronic characteristic. I_i is measured and J derived from this. On the graphic, we read the value of ξ corresponding to r = a, radius of the probe, which furnishes λ_D. In principle, we find the same value of λ_D if we repeat the operation for a different value of V_o. If Te is not known, we must proceed by successive approximation for several values of V.

Determination of g: adopting the hypothesis of Ref. 14, we define the sheath-plasma boundary by the condition $N_e = N_{eo}/2$ which corresponds to $\eta = 0.7$. For the same J as above, we then obtain the value of ξ corresponding to $r = a + g$, radius of the sheath. Evidently, the thickness g of the sheath depends on the polarization V_o of the probe. It should be noted that the theory of Bernstein and Rabinowitz [20] assumes that the probe radius is greater than a certain critical value below which certain particles would be "trapped" in the vicinity of the probe.

2. Experimental Findings of Static Measurements

We utilized the same central spherical probe to plot the Langmuir characteristics in a rather large range of discharges I_d between 55 mA below which the discharge is extinguished to 700 mA (above which the distribution of the plasma in the balloon is less homogenous). All these characteristics have the rate of those shown in Fig. 7, with very sharp saturation bends. Determined from the logarithmic slope after deducting the ion current, the temperature varies between 3,200 and 4,600° K. The plasma potential varies between -10 and - 7 V /18
from the anode utilized to establish a reference potential for the plasma (which is permissible in view of the large surface of contact between this electrode and the plasma [24]). Between 55 and 700 mA, the density varies very uniformly between 4 x 10^5 and 6.4 x 10^7 electron/cm.^{3}. The Debye distance was determined from these electronic and ionic characteristics. There exists excellent agreement above 400 mA but a rather marked divergence below 200 mA with as much as a factor of 2.5 for the very weak discharges. Fig. 8 summarizes the results obtained by static measurement.

c) h-f Measurements

We made the following verifications of the theory of the resonance probe:

1) resonance and antiresonance of I_{HF} and δI_{CC} occur generally for identical frequencies. We see in Fig. 9 to 12 that the trace of the experimental curves corresponds to the theoretical expectations. We further verified that, for a given density N_{eo}, only the resonance frequency shifts when the polarization V_o varies (cf. Figs. 9 to 12). Table I shows the typical results.

N_{eo} = 2,75.10^7 el/cm^3			N_{eo} = 3,50.10^7 el/cm^3			N_{eo} = 5.10^7 el/cm^3		
V_o	$\omega_R/2\pi$	$\omega_A/2\pi$	V_o	$\omega_R/2\pi$	$\omega_A/2\pi$	V_o	$\omega_R/2\pi$	$\omega_A/2\pi$
5,7 V	22 MHz	47 MHz	2,1 V	20 MHz	53 MHz	2 V	20 MHz	60 MHz
7,7 V	23	d°	3,8	20,8	d°	4	23,5	d°
			5	21,9	d°	7	26	d°
			7	24,1	d°			

Table I

2) antiresonance is manifested for $\omega_A = \omega_p$. Fig. 13 compares the density thus calculated with that obtained by the Langmuir probe. The difference between the two methods is less than 1%. /19

3) satisfactory agreement exists between the thickness of the ~~sheth~~ g estimated from the curves of Ref. 15 and that calculated from the value of the resonance and antiresonance frequency (Fig. 13). Accordingly, our findings show that the results deduced from the theory of Ref. 20 and from that of the resonance probe concur and justify the approximation utilized by assuming the sheath-plasma boundary defined by $N_e = N_{eo}/2$. Fig. 14 shows in addition the influence of density and of polarization V_o on the thickness of the sheath derived from the h-f measurements.

4) the values of collision frequency ν calculated from R through Rel. 12 were compared to those derived from the data of direct measurement of the effective cross section of collision given by Ref. 27. Fig. 15 manifests satisfactory agreement. Using the curves given in Ref. 27 is rather imprecise in view of the rapid variation of the effective cross section of electron collision in mercury as a function of energy at low energies.

5) we verified that the ratio R does pass through a maximum with the amplitude of resonance tending toward zero when V_o becomes very negative or on the contrary, when $V_o \to 0$. The maximum is actually located in $\omega_R = \frac{\omega_p}{\sqrt{3}}$ for discharges below 150mA. For stronger discharges, we were not able to verify Formula 15 because, in order to attain a sheath thickness g= a/2, a polarization was required such that the probe current would have been too weak for reading.

6) by varying, for a given value of V_o and N_{eo}, the amplitude of the h-f signal (Φ_o), we found that $|I_{HF}| \propto |\Phi_o|$ /20 and that $\delta I_{cc} \propto |\Phi_o|^2$, up to values of $|\Phi_o|$ comparable to $|V_o|$ (cf. Fig. 10).

REFERENCES /21

1. K. Takayama, H. Ikegami, S. Miyasaki: Phys. Rev. Letters vol. 5, p. 238, 1960.
2. Y.H. Ichikawa, H. Ikegami: Prog. Theoret. Phys., vol. 28, p. 315, 1962.
3. R.B. Cairns: Proc. Phys. Soc. vol. 82, p. 243, 1963.
4. G. Peter, G. Muller, H. Rabben: C.R. VIeme Conf. Int. sur les Phen. d'Ionis. dans les Gaz, 1963.
5. H. Mayer: C.R. VIeme Conf. Int. sur les Phen. d'Ionis. dans les Gaz, 1963.
6. H.W. Wimmel: Institute for plasma phys. Report No. 6/11, 1963.
7. P. Vandenplas, R. Gould: C.R. de la Veme Conf. Int. sur les Phen. d'Ionis. dans les Gaz, vol. 2, p. 1470, 1961.
8. P. Vandenplas, R. Gould: Physica, vol. 28, p. 357, 1962.
10. A. Messiaen, P. Vandenplas: Physica, vol. 30, p. 303,1964.
11. S. M. Levitskii, J.P. Shashurin: Sov. Phys. Tech. Phys.,vol. 8, p. 319, 1963.
12. R.S. Harp, F.W. Crawford: J. of Applied Phys. vol. 35, p.12 1964.
13. J. Pavkovich, G.S. Kino: C.R. de la VIeme Conf. Int.sur les Phen. d'Ionis. dans les Gaz, 1963.
14. A. Messiaen: C.R. Acad. Sc. Paris, vol. 259, pages 1710-13 1964, and unpublished internal reports.
15. F.F. Chen: J. of Nuclear Energy Part C, vol.7, p. 47, 1965.
16. D. Lepechinsky, P. Rolland, J. Taillet: Note aux C.R. Acad. Sc. Paris, vol. 261, pages 663-664, 1965.
17. P. Rolland: C.R. Acad. Sc. (to be published).
18. G. Von Gierke, G. Muller, G. Peter, H. Rabben: Z. Natur- /22 forschung, vol. 19a, p. 1107, 1964.
19. T. Dote, T. Ichimiya: J. of Applied Phys., vol. 36, p. 1866, 1965.
20. I. B. Bernstein, I. Rabinowitz: Phys. of Fluids, vol. 2, p. 112, 1959
21. J. Allen, R. Boyd, P. Reynolds: Proc. Phys. Soc., vol. 70B, p.297, 1957.
22. A. Caruso, A. Cavaliere: Il Nuovo Cimento, vol. 26, p.1389, 1962.
23. S. Self: Stanford University, Microwave Lab. Report No. 1056, 1963.
24. A. Boschi, F. Magistrelli: Il Nuovo Cimento, vol. 29, p. 487, 1963.

25. R.C.A. Review, vol 28, 2, p. 200, 1957 (R.Honig).
26. L. B. Loeb: Basic Processes of gaseous electronics, 1960.
27. C. McCutchen: Phys. Rev., vol. 112, p. 1848, 1958.
28. J. Taillet: These, 1964.
29. P. Vandenplas, A. Messiaen: Plasma Physics, J. of Nuclear Energy Part C, vol. 6, p. 459, 1964.
30. W. Leavens: Physics Letters, vol. 15, 310, 1965.

Translated for the National Aeronautics and Space Administration by the Translation and Interpretation Division, Institute of Modern Languages, under Contract NASw-1693.

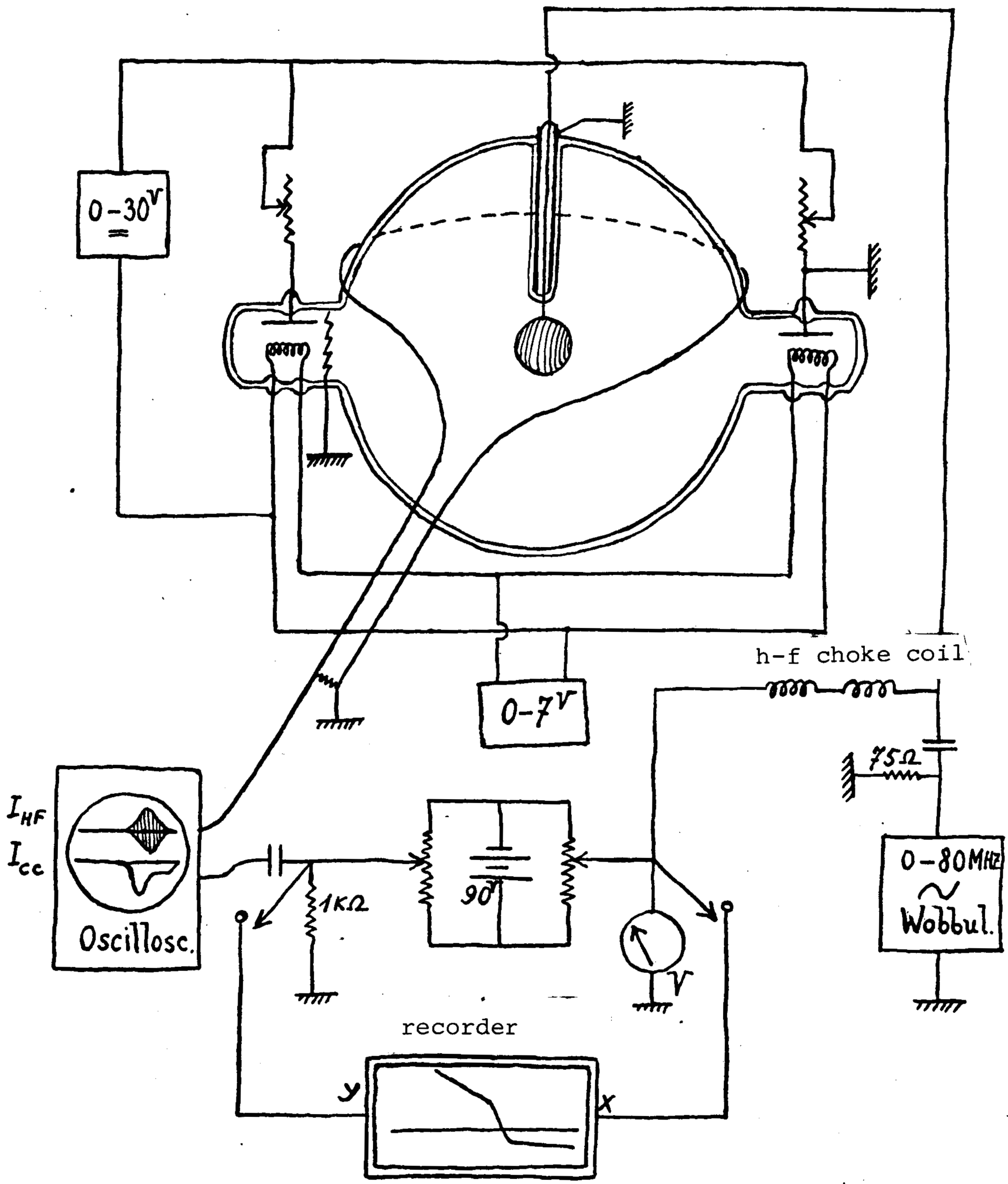
0-30V
0-7V
h-f choke coil
75Ω
0-80MHz
Wobbul.
I_{HF}
I_{cc}
Oscillosc.
1KΩ
90V
V
recorder
y
x

- Fig. 4 -

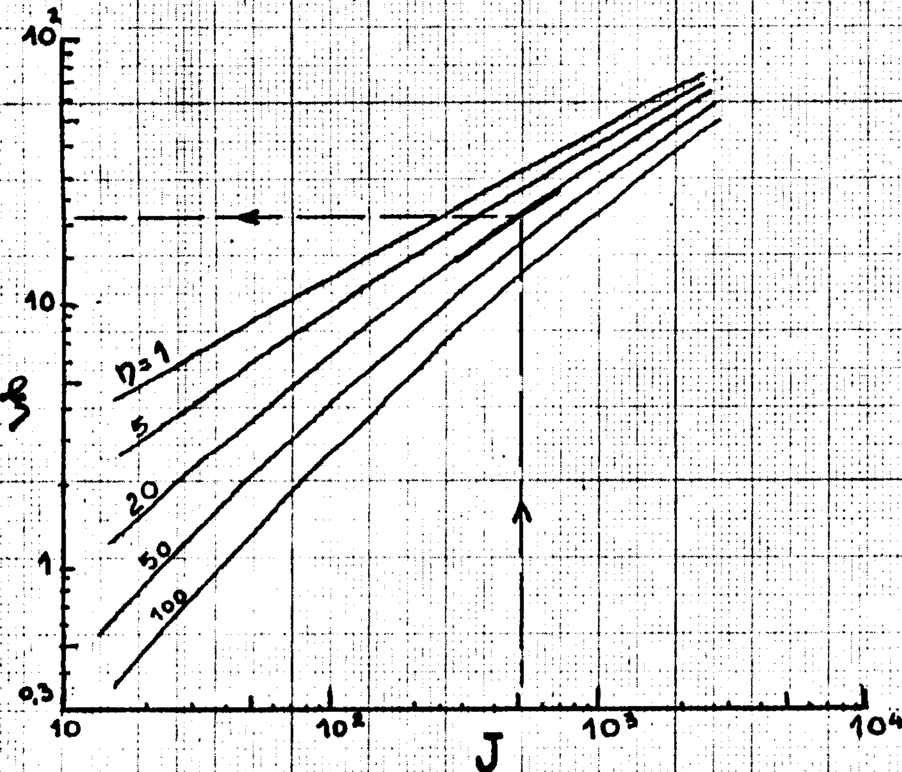

10^2
10
1
0,3
ξ
$\eta=1$
5
20
50
100
10
10^2
10^3
10^4
J

FIG. 5

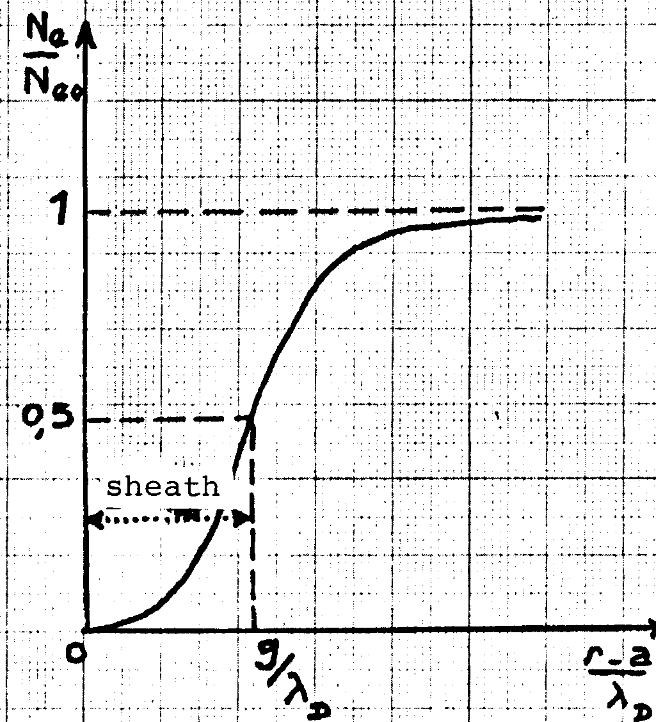

$\frac{N_e}{N_{eo}}$
1
0,5
sheath
0
g/λ_D
$\frac{r-a}{\lambda_D}$

Fig: 6

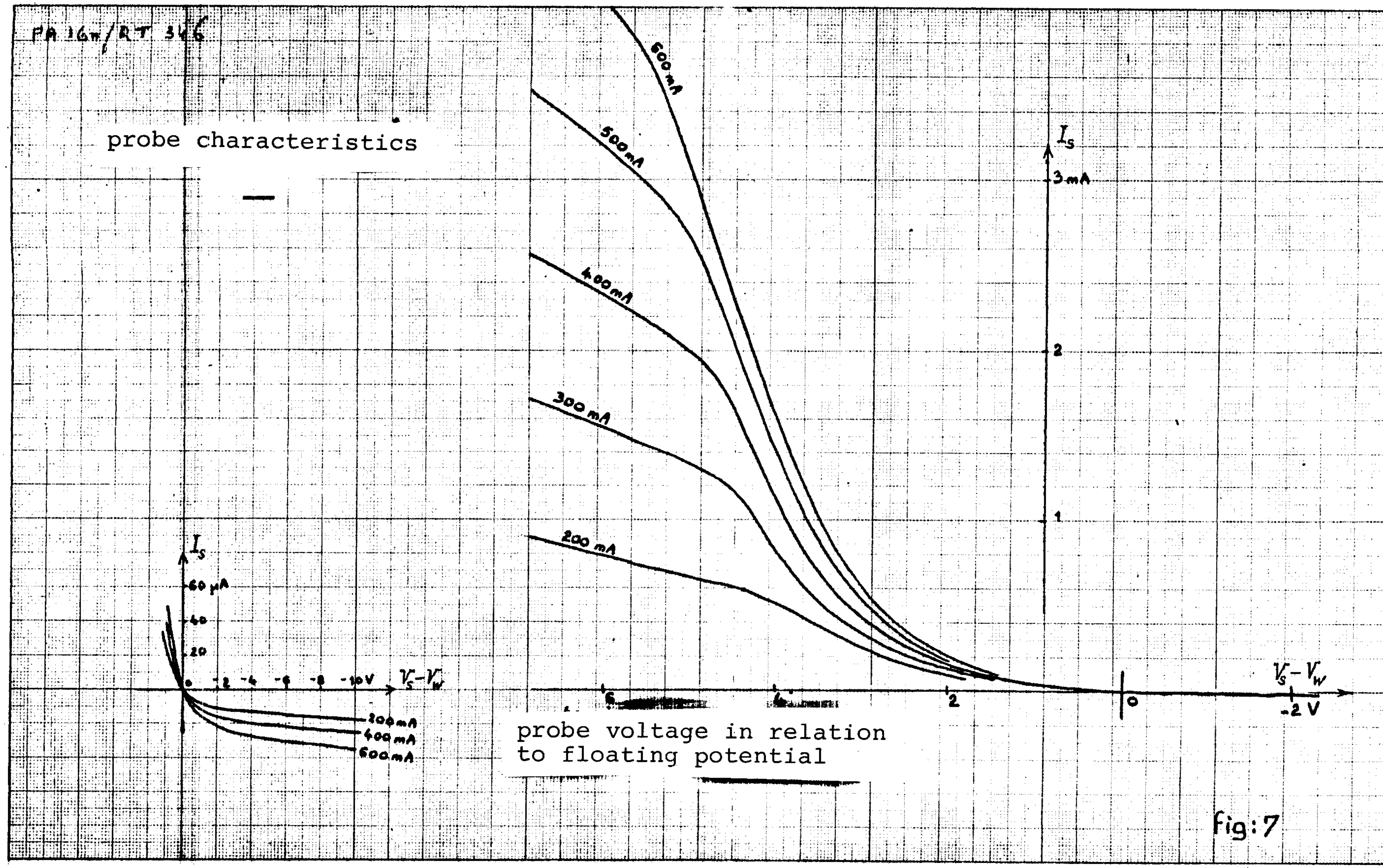
FA 16π/RT 346
probe characteristics
I_s
60 μA
40
20
0
-2
-4
-6
-8
-10 V
$V_s - V_W$
200 mA
400 mA
600 mA
500 mA
300 mA
3 mA
2
1
6
4
0
-2 V
probe voltage in relation to floating potential

Fig: 7

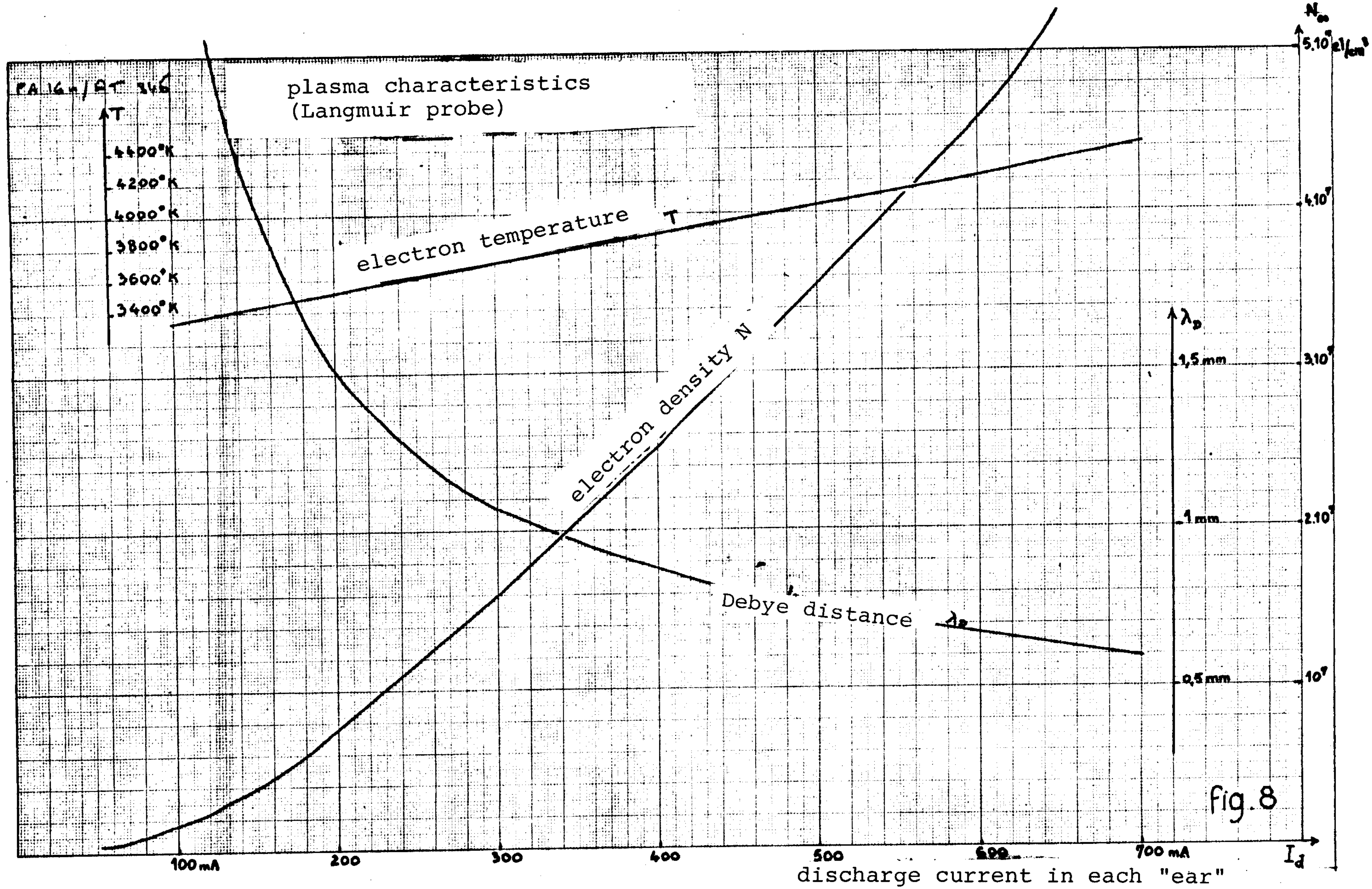
PA 164/AT 346
plasma characteristics
(Langmuir probe)
T
4400°K
4200°K
4000°K
3800°K
3600°K
3400°K
electron temperature T
electron density N
Debye distance λ_D
N_{eo}
5.10^7 el/cm³
4.10^7
3.10^7
2.10^7
10^7
λ_D
1,5 mm
1 mm
0,5 mm
100 mA
200
300
400
500
600
700 mA
I_d
discharge current in each "ear"

fig. 8

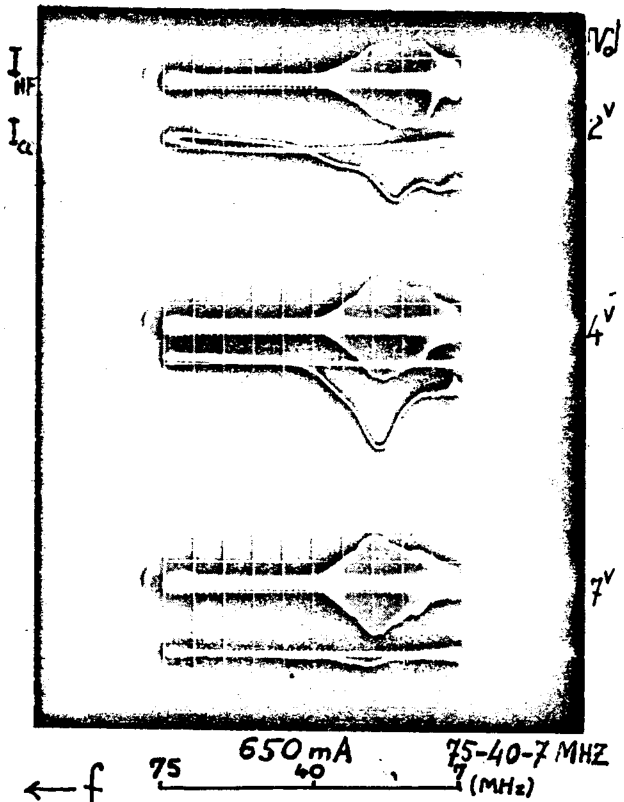

- Fig. 9 -

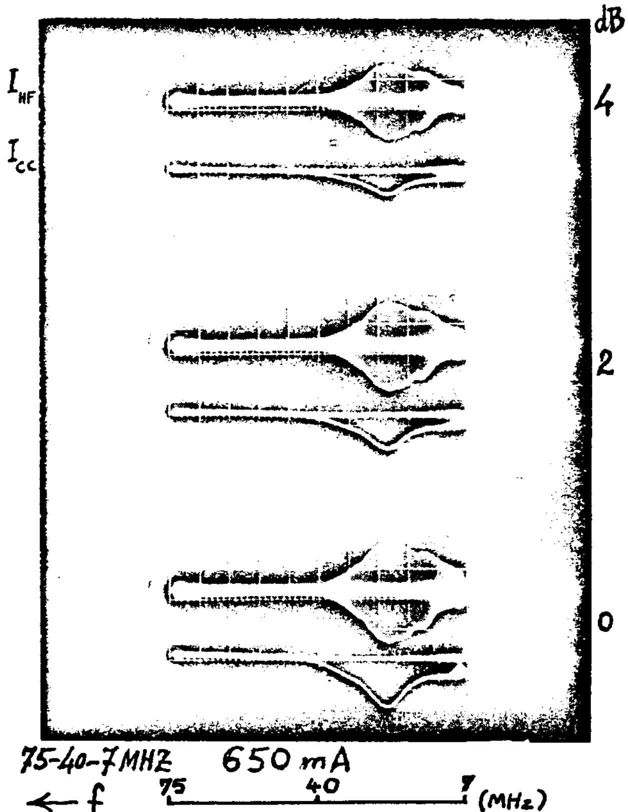

- Fig. 10 -

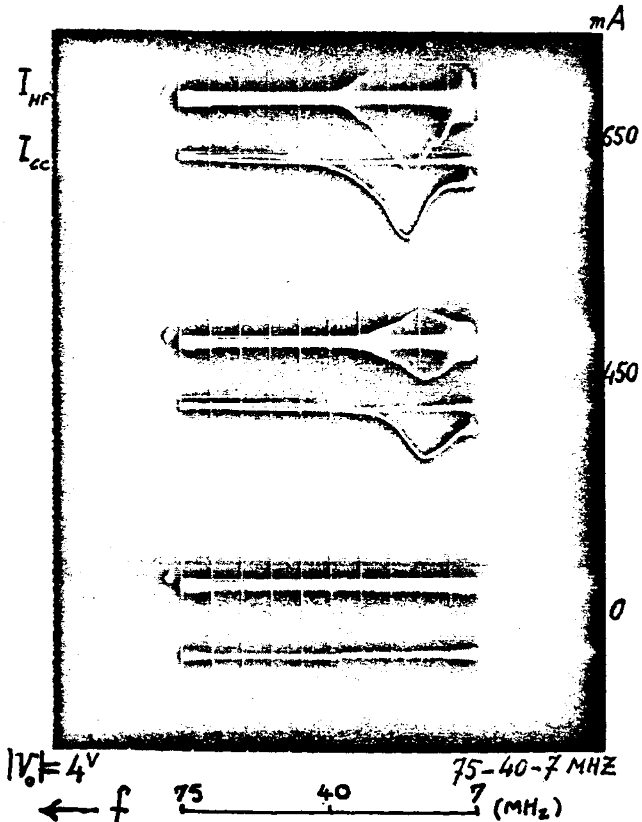

- Fig. 11 -

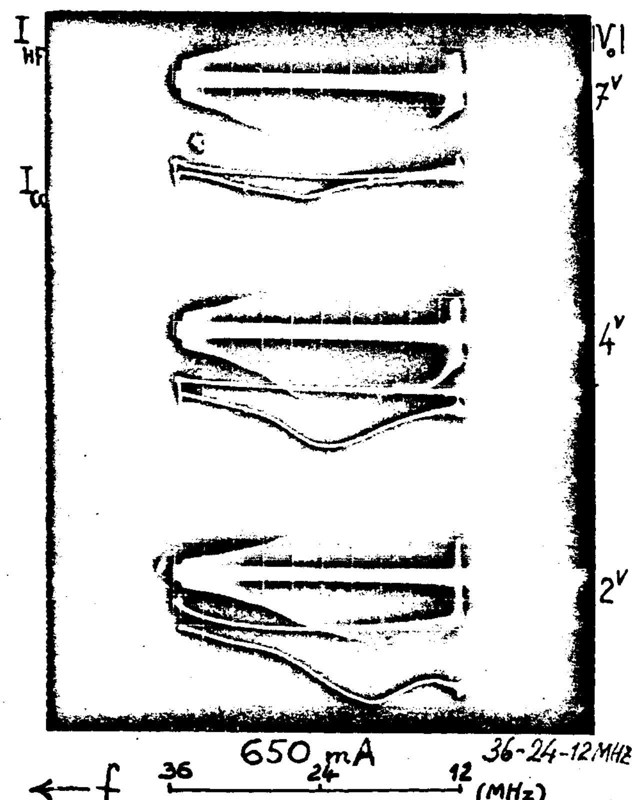

- Fig. 12 -

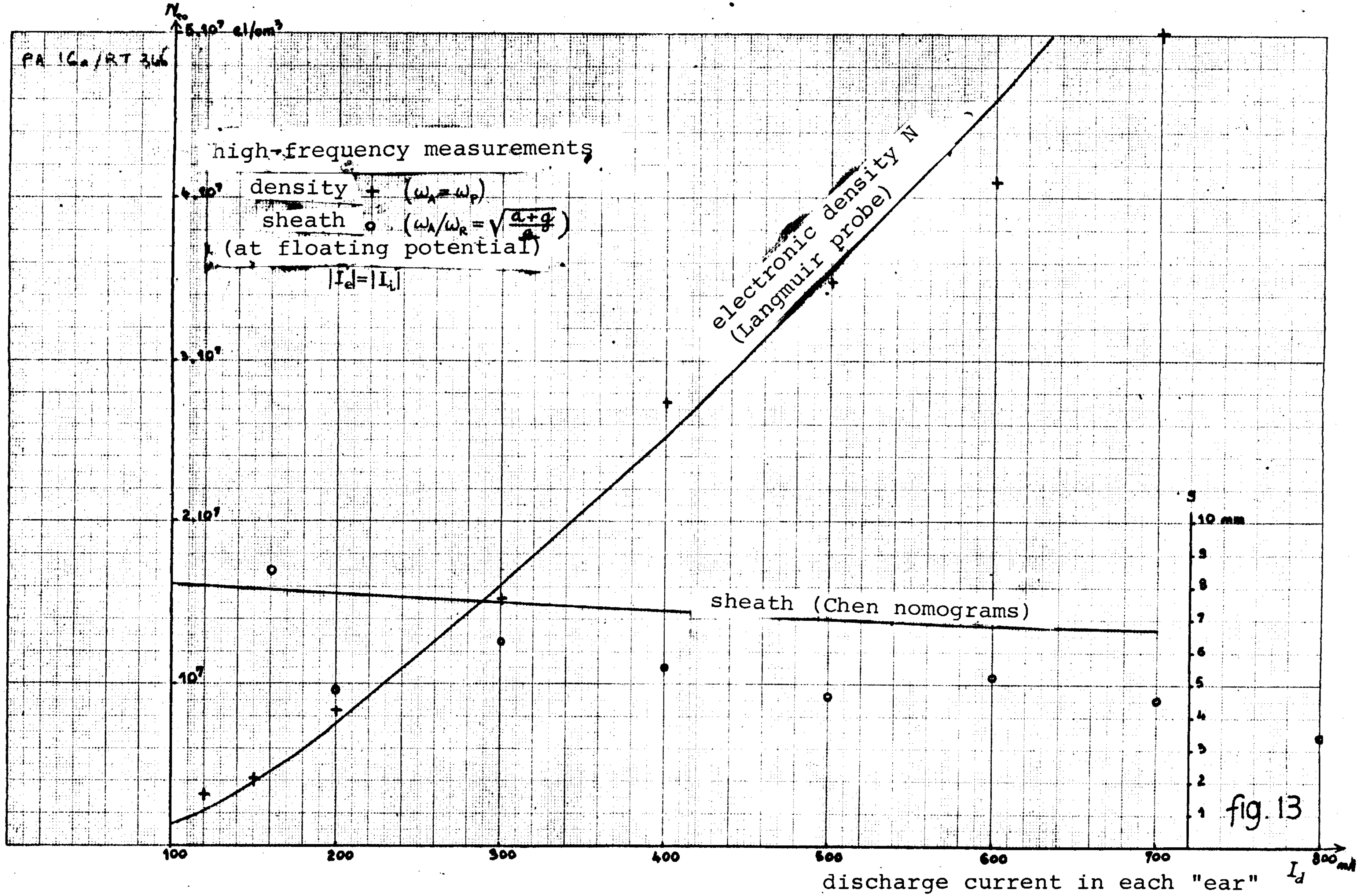
PA ICa / RT 366
N_{eo}
5.10^7 el/cm³
4.10^7
3.10^7
2.10^7
10^7
high-frequency measurements
density + ($\omega_A = \omega_p$)
sheath o ($\omega_A/\omega_R = \sqrt{\frac{a+g}{a}}$)
(at floating potential)
$|I_e| = |I_i|$
electronic density N
(Langmuir probe)
sheath (Chen nomograms)
S
10 mm
9
8
7
6
5
4
3
2
1
100
200
300
400
500
600
700
800 mA
I_d
discharge current in each "ear"
fig. 13

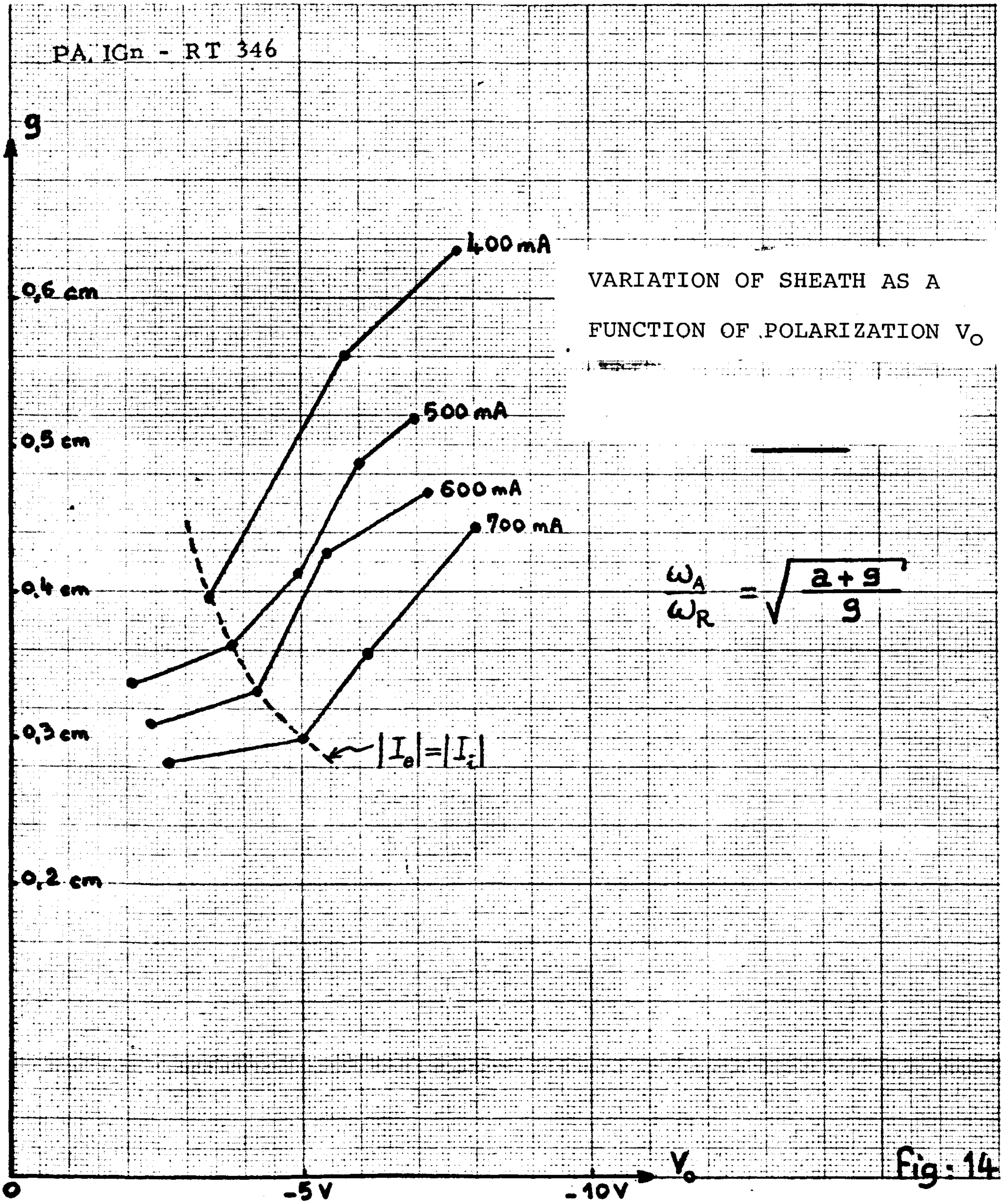

PA. IGn - RT 346
g
0,6 cm
0,5 cm
0,4 cm
0,3 cm
0,2 cm
400 mA
500 mA
600 mA
700 mA
$|I_e| = |I_i|$
VARIATION OF SHEATH AS A FUNCTION OF POLARIZATION V_o
$$\frac{\omega_A}{\omega_R} = \sqrt{\frac{a+g}{g}}$$
0
-5 V
-10 V
V_o

Fig: 14

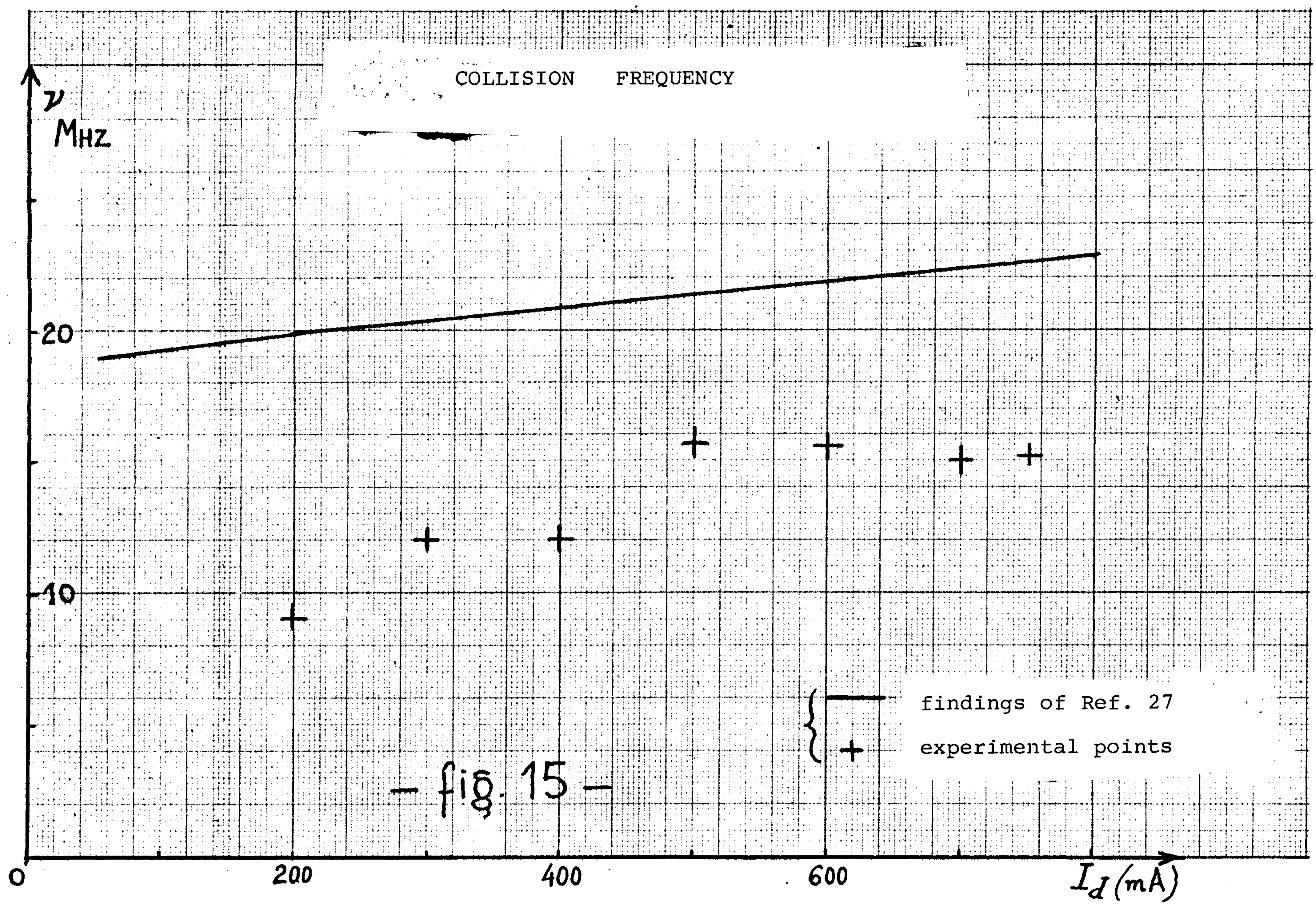
COLLISION FREQUENCY
ν
MHZ
20
10
0
200
400
600
Id (mA)
findings of Ref. 27
experimental points

– fig. 15 –

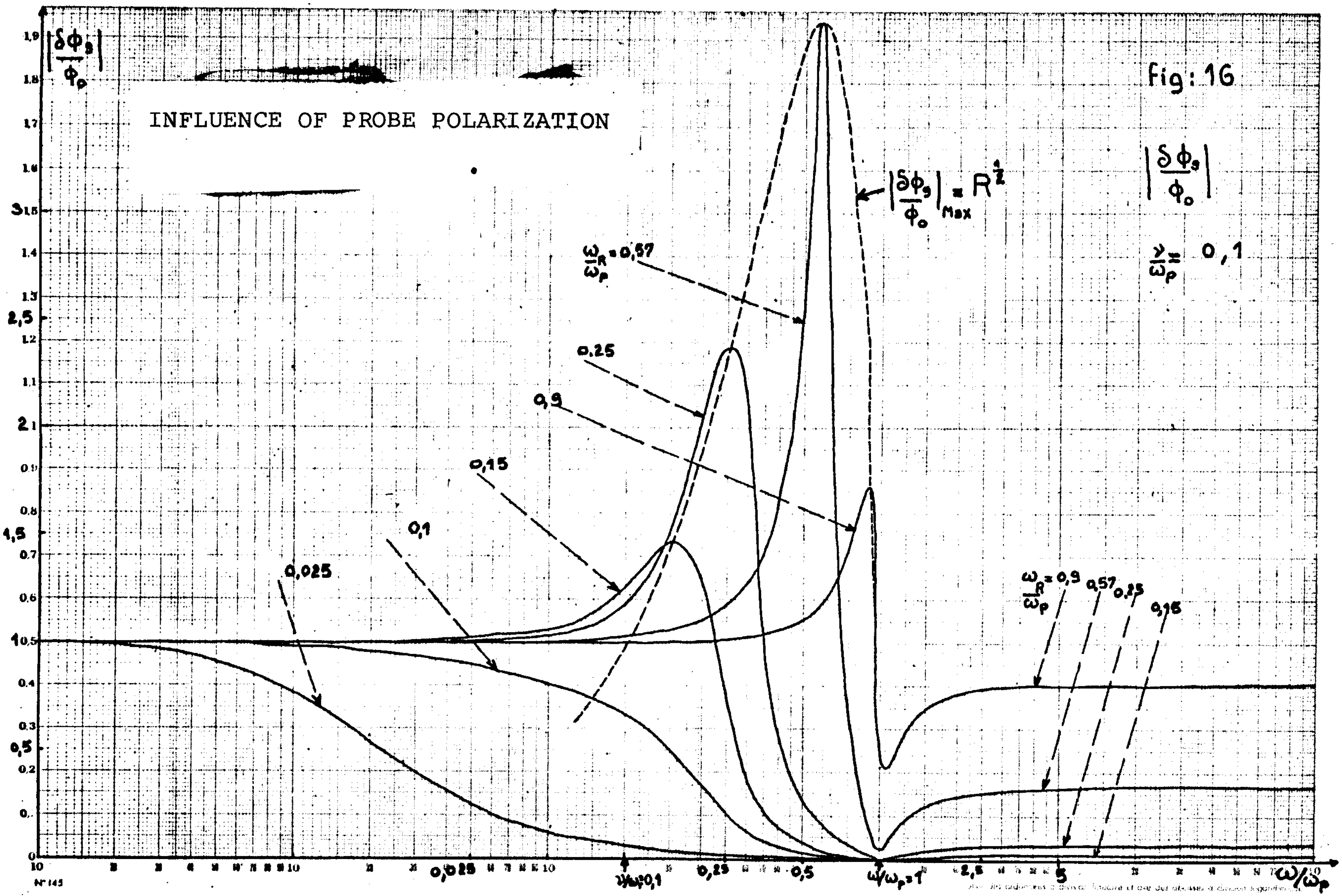

INFLUENCE OF PROBE POLARIZATION
Fig: 16
$\left|\frac{\delta\phi_s}{\phi_o}\right|$
$\frac{\nu}{\omega_p} = 0,1$
$\left|\frac{\delta\phi_s}{\phi_o}\right|_{Max} = R^{\frac{1}{2}}$
$\frac{\omega_R}{\omega_p} = 0,57$
0,25
0,9
0,15
0,1
0,025
$\frac{\omega_R}{\omega_p} = 0,9$ 0,57 0,25 0,15
ω/ω_p
$\omega/\omega_p = 1$
$\nu/\omega_p = 0,1$